

Supporting Information

Fluorinated pyrazine-based D-A conjugated polymers for efficient non-fullerene polymer solar cells

*Kai Chen,[‡] *^{a,b,c} Ruijie Ma,^{‡,b,c} Tao Liu,^{*b,c} Zhenghui Luo,^{b,c} Xiaopeng Xu,^{b,c} Qiutang Wang,^a Yuzhong Chen,^{b,c} Yiqun Xiao,^d Xinhui Lu,^d He Yan,^{*b,c}*

^a College of Pharmacy, Xi'an Jiaotong University, No.76 Yanta West Road, Xi'an, Shaanxi Province 710061, People's Republic of China.

E-mail addresses: chenkai1816@mail.xjtu.edu.cn (K. Chen)

^b Department of Chemistry and Hong Kong Branch of Chinese National Engineering Research Center for Tissue Restoration & Reconstruction, Hong Kong University of Science and Technology, Clear Water Bay, Kowloon, Hong Kong

E-mail addresses: liutaozhx@ust.hk (T. Liu), hyan@ust.hk (H. Yan)

^c Hong Kong University of Science and Technology-Shenzhen Research Institute, No. 9 Yuexing first RD, Hi-tech Park, Nanshan, Shenzhen 518057, P. R. China.

^d Department of Physics, The Chinese University of Hong Kong, New Territories 999077, Hong Kong

[‡] These authors contributed equally to this work.

Experimental Procedures

Materials and Instruments:

All reagents and chemicals were purchased commercially and used directly without further purification unless otherwise stated. Anhydrous toluene and tetrahydrofuran (THF) were distilled from Na/benzophenone under argon flow. Unless otherwise stated, all reactions were carried out under inert atmosphere using standard Schlenk-line techniques. ^1H and ^{13}C NMR spectra were recorded on Bruker Ascend 400 MHz spectrometer using CDCl_3 as the deuterium solvent. Elemental analyses (EAs) of compounds were conducted in the Center of Analysis and Characterization at Shenzhen University (Shenzhen, China). High-resolution mass spectrometry was obtained on Thermo Scientific TM Q-Exactive, and polymer molecular weight was characterized using a high-temperature gel permeation chromatography (GPC, Agilent PL-GPC220) at 150 °C with 1,2,4-trichlorobenzene as the eluent and polystyrenes as the standards. UV-vis absorption spectra of polymer solutions and films were recorded on a Shimadzu UV-3600 UV-VIS-NIR spectrophotometer. Cyclic voltammetry measurements of BDT-PY and BDT-FPY films were carried out under argon using a CHI760 Voltammetry Workstation with a N_2 -saturated tetra(n-butyl)ammonium hexafluorophosphate (Bu_4NPF_6 , 0.1 M) solution in acetonitrile (CH_3CN) as the supporting electrolyte. A platinum disk working electrode, a platinum wire counter electrode, and a silver wire reference electrode were employed, and the ferrocene/ferrocenium (Fc/Fc^+) redox couple was used as the reference for all measurements with a scanning rate of 50 mV s^{-1} . Thermogravimetric analysis (TGA)

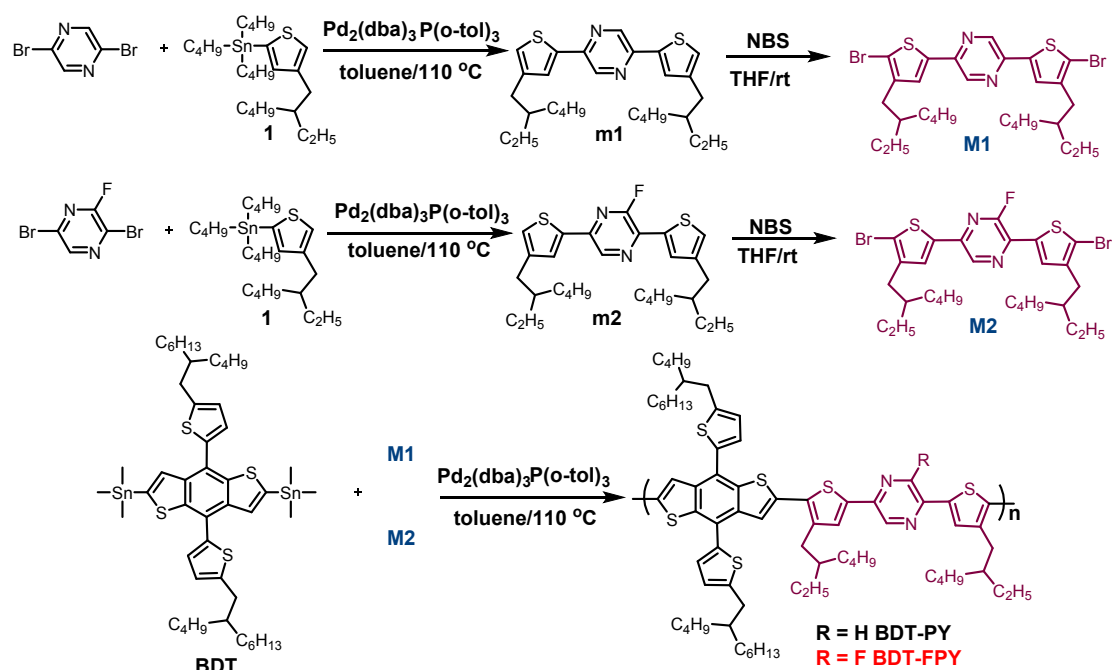
of polymers was carried out with a METTLER TOLEDO (TGA 1 STARe System) apparatus at a heating ramp of 10 °C min⁻¹ under N₂ atmosphere.

The external quantum efficiency (EQE) spectra of solar cells were recorded by a QE-R3011 measurement system (Enli Technology, Inc.). AFM measurements were obtained by using a Dimension Icon AFM (Bruker) in a tapping mode. The grazing incidence X-ray scattering (GIWAXS) measurement was carried out with a Xeuss 2.0 SAXS/WAXS laboratory beamline using a Cu X-ray source (8.05 keV, 1.54 Å) and a Pilatus3R 300K detector. The incident angle was 0.2°. The samples for GIWAXS measurements were fabricated on silicon substrates using the same recipe for the devices. The electron and hole mobility were measured by using the method of space-charge limited current (SCLC) for electron-only devices with the structure of ITO/ZnO/active layer/ZrAcAc/Al and hole-only devices with the structure of ITO/MoO₃/active layer/MoO₃/Al. The charge carrier mobility was determined by fitting the dark current to the model of a single carrier SCLC according to the equation: $J = 9\varepsilon_0\varepsilon_r\mu V^2/8d^3$, where J is the current density, d is the film thickness of the active layer, μ is the charge carrier mobility, ε_r is the relative dielectric constant of the transport medium, and ε_0 is the permittivity of free space. $V = V_{\text{app}} - V_{\text{bi}}$, where V_{app} is the applied voltage, V_{bi} is the offset voltage. The carrier mobility can be calculated from the slope of the $J^{1/2} \sim V$ curves.

Fabrication and characterization of polymer solar cells.

Solar cells were fabricated in a conventional device configuration of ITO/PEDOT:PSS/donors:MeIC/Zracac/Al. The ITO substrates were first scrubbed by detergent and then sonicated with deionized water, acetone and isopropanol subsequently, and dried overnight in an oven. The glass substrates were treated by UV-Ozone for 30 min before use. PEDOT:PSS (Heraeus Clevious P VP AI 4083) was spin-cast onto the ITO substrates at 4000 rpm for 30 s, and then dried at 150 °C for 15 min in air. The donor: acceptor blends (1:1 weight ratio) were dissolved in chloroform (the total concentration of blend solutions was 16 mg mL⁻¹ for all blends and DIO was chosen as additive whose volume ratio was 0.25%) and stirred overnight in room temperature in a nitrogen-filled glove box. The blend solution was spin-cast at 3000 rpm for 30 s. Active layers were annealed on a 100 °C hotplate for 3 minutes after being coated. A thin Zracac layer was coated on the active layer, followed by the deposition of AL (100 nm) (evaporated under 5×10⁻⁵ Pa through a shadow mask). The optimal active layer thickness measured by a Bruker Dektak XT stylus profilometer was about 105 nm. The current density-voltage (J-V) curves of all encapsulated devices were measured using a Keithley 2400 Source Meter in air under AM 1.5G (100 mW cm⁻²) using a Newport solar simulator. The light intensity was calibrated using a standard Si diode (with KG5 filter, purchased from PV Measurement to bring spectral mismatch to unity). Optical microscope (Olympus BX51) was used to define the device area (5.9 mm²). EQEs were measured using an Enlitech QE-S EQE system equipped with a standard Si diode. Monochromatic light was generated from a Newport 300W lamp source.

Chemical Synthesis:



Scheme S1. The synthetic routes of BDT-PY and BDT-FPY.

m1: In a 250 mL Schlenk tube, the mixture of 2,5-dibromopyrazine (1.4 g, 5.9 mmol, 1.0 eq), 4-(2-ethylhexyl)-2-(tributylstannyl)thiophene (5.0 g, 13.4 mmol, 2.27 eq), $\text{Pd}_2(\text{dba})_3$ (0.5 g, 0.5 mmol, 8.47% eq), tri(o-tolyl)phosphine (0.4 g, 1.3 mmol, 22% eq) in toluene (50 mL) was stirred at 110 °C overnight, under the protection of N_2 . After cooling the solution to room temperature, the reaction mixture was poured into a 250 mL separatory funnel to separate the organic phase, and using CH_2Cl_2 to extract the aqueous phase. Then, the combined organic phase was dried by MgSO_4 and concentrated by rotary evaporator. At last, the residue was purified by a silica gel column (Petroleum ether / CH_2Cl_2 = 1/1, v/v) to afford **m1** as a yellow solid (1.55 g, 56% yield). ^1H NMR (400 MHz, CDCl_3 , TMS), δ (ppm): 8.81 (s, 2H), 7.46 (s, 2H), 7.03 (s, 2H), 2.58 (d, J = 4.0 Hz, 4H), 1.62-1.59 (m, 2H), 1.29 (m, 16H), 0.91-0.89 (m,

12H). ^{13}C NMR (150 MHz, CDCl_3 , TMS), (ppm): 145.97, 143.58, 140.72, 139.36, 127.05, 124.28, 40.29, 34.57, 32.43, 28.86, 25.59, 23.04, 14.15, 10.83.

M1: The compound **m1** (1.64 g, 3.5 mmol, 1.0 eq) and N-bromosuccinimide (2.5 g, 14.0 mmol, 4.0 eq) was added into a 300 mL round-bottom flask with THF 50 mL and the mixture was stirred at room temperature out of light for 48 h. Then, the reaction was concentrated by rotary evaporator, and the residue was purified by a silica gel column (Petroleum ether / CH_2Cl_2 = 1/1, v/v) to afford compound **M1** as a yellow solid (1.38g, 63% yield). ^1H NMR (400 MHz, CDCl_3 , TMS), δ (ppm): 8.72 (s, 2H), 7.30 (s, 2H), 2.53 (d, J = 4.0 Hz, 4H), 1.67-1.63 (m, 2H), 1.37-1.29 (m, 16H), 0.92-0.88 (m, 12H). ^{13}C NMR (150 MHz, CDCl_3 , TMS), (ppm): 145.38, 143.00, 140.51, 138.88, 126.45, 113.95, 39.97, 33.95, 32.45, 28.77, 25.67, 23.06, 14.14, 10.85. MALDI-TOF MS (m/z) for $\text{C}_{28}\text{H}_{38}\text{Br}_2\text{N}_2\text{S}_2$: 626.08.

m2: In a 250 mL Schlenk tube, the mixture of 2,5-dibromo-3-fluoropyrazine (1.5 g, 5.9 mmol, 1.0 eq), 4-(2-ethylhexyl)-2-(tributylstannyl)thiophene (5.0 g, 13.4 mmol, 2.27 eq), $\text{Pd}_2(\text{dba})_3$ (0.5 g, 0.5 mmol, 8.47% eq), tri(o-tolyl)phosphine (0.4 g, 1.3 mmol, 22% eq) in toluene (50 mL) was stirred at 110 °C overnight, under the protection of N_2 . After cooling the solution to room temperature, the reaction mixture was poured into a 250 mL separatory funnel to separate the organic phase, and using CH_2Cl_2 to extract the aqueous phase. Then, the combined organic phase was dried by MgSO_4 and concentrated by rotary evaporator. At last, the residue was purified by a silica gel

column (Petroleum ether / CH₂Cl₂ = 1/1, v/v) to afford **m2** as a yellow solid (1.7 g, 61% yield). ¹H NMR (400 MHz, CDCl₃, TMS), δ (ppm): 8.68 (d, *J* = 4.0 Hz, 1H), 7.64 (s, 1H), 7.51(s, 1H), 7.09 (s, 1H), 7.05 (s, 1H), 2.59-2.56 (m, 4H), 1.62-1.59 (m, 2H), 1.34-1.29 (m, 16H), 0.92-0.89 (m, 12H). ¹³C NMR (150 MHz, CDCl₃, TMS), (ppm): 155.38, 153.68, 143.70, 143.33, 143.28, 138.73, 137.51, 137.44, 136.26, 136.24, 134.70, 134.53, 130.58, 130.50, 128.31, 125.22, 124.96, 40.24, 34.57, 34.48, 32.40, 28.81, 25.57, 23.03, 14.11, 10.79. ¹⁹F NMR (376.5 MHz, CDCl₃) δ -73.56.

M2: The compound **m2** (1.7 g, 3.5 mmol, 1.0 eq) and N-bromosuccinimide (2.5 g, 14.0 mmol, 4.0 eq) was added into a 300 ml round-bottom flask with THF 50 mL and the mixture was stirred at room temperature out of light for 48 h. Then, the reaction was concentrated by rotary evaporator. , and the residue was purified by a silica gel column (Petroleum ether / CH₂Cl₂ = 1/1, v/v) to afford compound **M2** as a yellow solid (1.5g, 67% yield). ¹H NMR (400 MHz, CDCl₃, TMS), δ (ppm): 8.62 (d, *J* = 4.0 Hz, 1H), 7.47 (s, 1H), 7.36 (s, 1H), 2.54-2.52 (m, 4H), 1.66-1.64 (m, 2H), 1.36-1.30 (m, 16H), 0.93-0.88 (m, 12H). ¹³C NMR (150 MHz, CDCl₃, TMS), (ppm): 155.23, 153.52, 143.26, 142.68, 142.58, 138.41, 137.28, 135.92, 134.22, 134.05, 130.25, 130.17, 127.84, 115.43, 114.74, 39.96, 39.91, 33.99, 33.90, 32.45, 32.43, 28.76, 28.74, 25.68, 23.06, 14.14, 10.84. ¹⁹F NMR (376.5 MHz, CDCl₃) δ -73.50. MALDI-TOF MS (m/z) for C₂₈H₃₇Br₂FN₂S₂: 645.08.

BDT-PY: To a 25 mL reaction tube equipped with a stirring bar was added the monomer M1 (62.6 mg, 0.1 mmol, 1.0 eq), the distannylated monomer BDT (101.7 mg, 0.1 mmol, 1.0 eq), Pd₂(dba)₃ (1.37 mg, 0.0015 mmol, 1.5% eq), P(o-tolyl)₃ (3.65 mg, 0.012 mmol, 12% eq), and anhydrous toluene (4.0 mL). The reaction tube was purged with argon and sealed under argon flow. The tube was heated to 110 °C for 24 h. After cooled to room temperature, the reaction solution was added dropwise into 80 mL methanol under vigorous stirring and stirred for 1 h. The precipitate was filtrated and purified by a silica gel column (CHCl₃) to yield the product polymer as a purplish-red solid (108.8 mg, 94%). Due to the limited solubility of this polymer in various deuterium solvents, high quality ¹H NMR spectrum cannot be measured. Calcd for C₇₀H₉₆N₂S₆: C, 72.61; H, 8.36; N, 2.42, Found: C, 72.57; H, 8.30, N, 2.38. Molecular weight: Mn = 37.5 kDa, PDI = 2.1.

BDT-FPY: To a 25 mL reaction tube equipped with a stirring bar was added the monomer M2 (64.4 mg, 0.1 mmol, 1.0 eq), the distannylated monomer BDT (101.7 mg, 0.1 mmol, 1.0 eq), Pd₂(dba)₃ (1.37 mg, 0.0015 mmol, 1.5% eq), P(o-tolyl)₃ (3.65 mg, 0.012 mmol, 12% eq), and anhydrous toluene (4.0 mL). The reaction tube was purged with argon and sealed under argon flow. The tube was heated to 110 °C for 1 h. After cooled to room temperature, the reaction solution was added dropwise into 80 mL methanol under vigorous stirring and stirred for 1 h. The precipitate was filtrated and purified by a silica gel column (CHCl₃) to yield the product polymer as a dark-red solid (104.6 mg, 89%). Due to the limited solubility of this polymer in various deuterium

solvents, high quality ^1H NMR spectrum cannot be measured. Calcd for $\text{C}_{70}\text{H}_9\text{FN}_2\text{S}_6$: C, 71.50; H, 8.14; N, 2.38, Found: C, 71.45; H, 8.09, N, 2.40. Molecular weight: $M_n = 59.4$ kDa, PDI = 2.3.

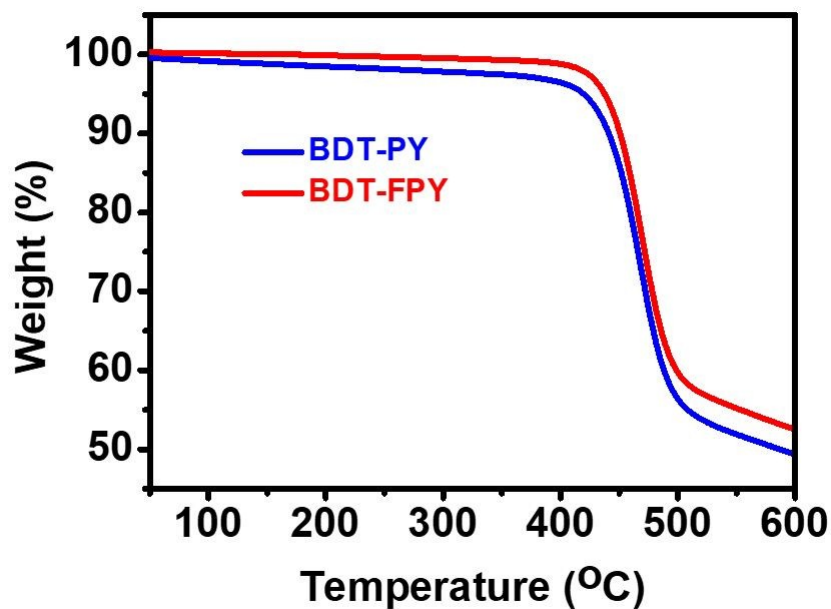


Fig. S1. Thermogravimetric analysis (heating ramp: $10\text{ }^\circ\text{C min}^{-1}$) of polymers BDT-PY and BDT-FPY.

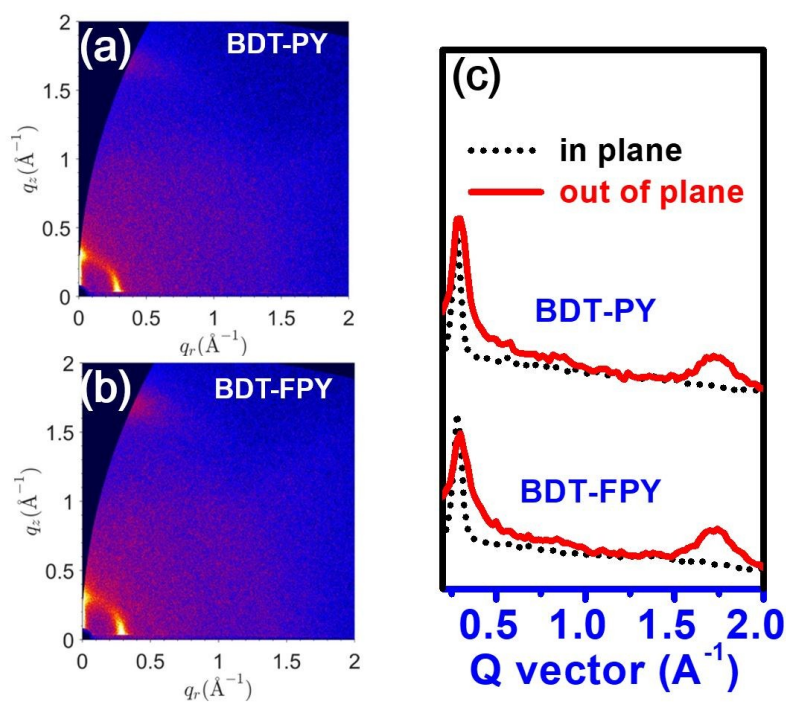


Fig. S2 (a) and (b): Two-dimensional GIWAXS patterns of BDT-PY and BDT-FPY neat films; (c): GIWAXS intensity profiles of BDT-PY and BDT-FPY films along the in-plane (black lines) and out-of-plane (red lines) directions.

Table S1. GIWAXS test performance parameters of the BDT-PY, BDT-FPY, BDT-PY : MeIC and BDT-PY : MeIC pure films and the related as-cast or thermal annealed blend films.

	in plane			out of plane		
	location (\AA^{-1})	d-spacing (\AA)	CCL (\AA)	location (\AA^{-1})	d-spacing (\AA)	CCL (\AA)
BDT-PY	0.28	22.4	115.3	1.72	3.65	53.3
BDT-FPY	0.28	22.4	110.8	1.72	3.65	56.7
BDT-PY : MeIC	0.28	22.4	81.4	1.76	3.56	21.8
BDT-FPY : MeIC	0.29	21.7	70.0	1.76	3.56	23.0

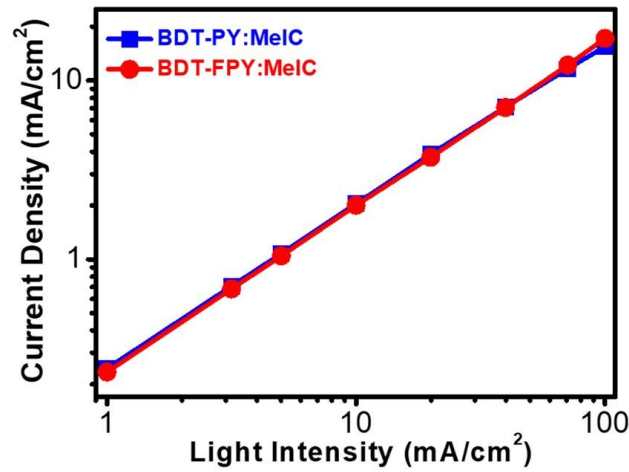


Fig. S3 Light intensity dependence of J_{SC} of the devices based on BDT-PY : MeIC and BDT-PY : MeIC.

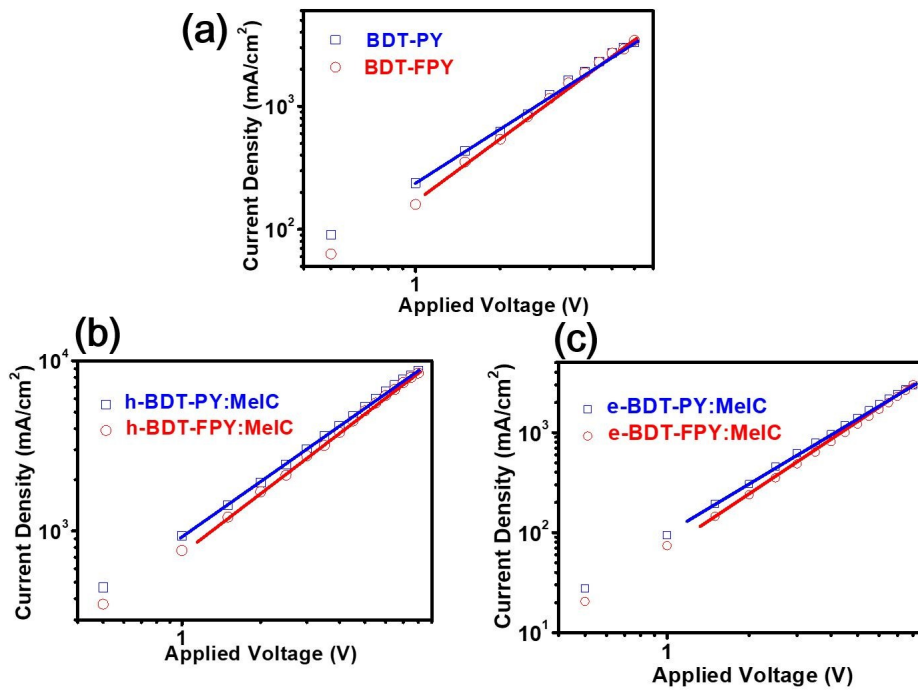


Fig. S4 The J - V curves of (a) the hole-only devices with the structure of ITO/MoO₃/donor/MoO₃/Al; (b) the hole-only devices with the structure of ITO/MoO₃/donor : MeIC /MoO₃/Al and (c) the electron-only devices with the structure of ITO/ZnO/ donor : MeIC /ZrAcAc/Al according to the SCLC model.

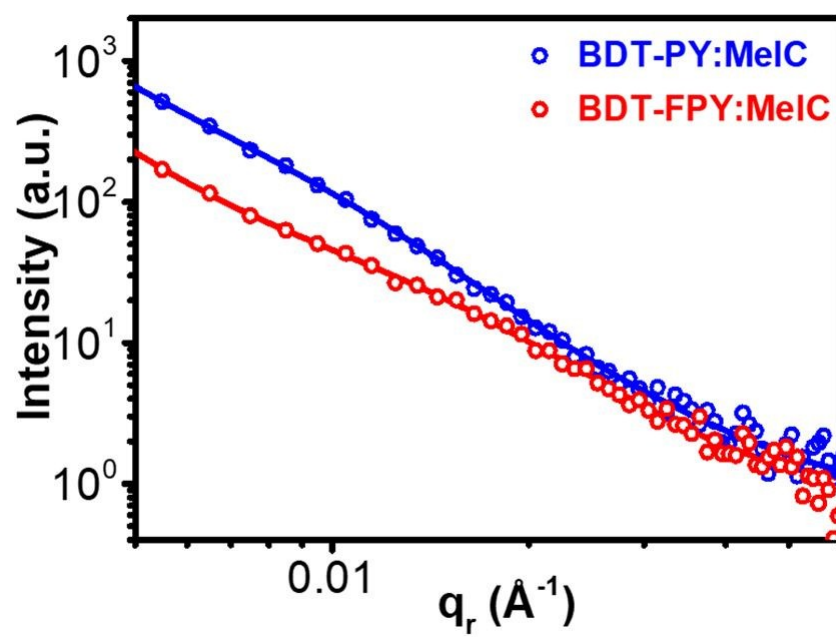


Fig. S5 GISAXS intensity profiles and best fittings along the in-plane direction.

NMR and Mass Spectra of Compounds:

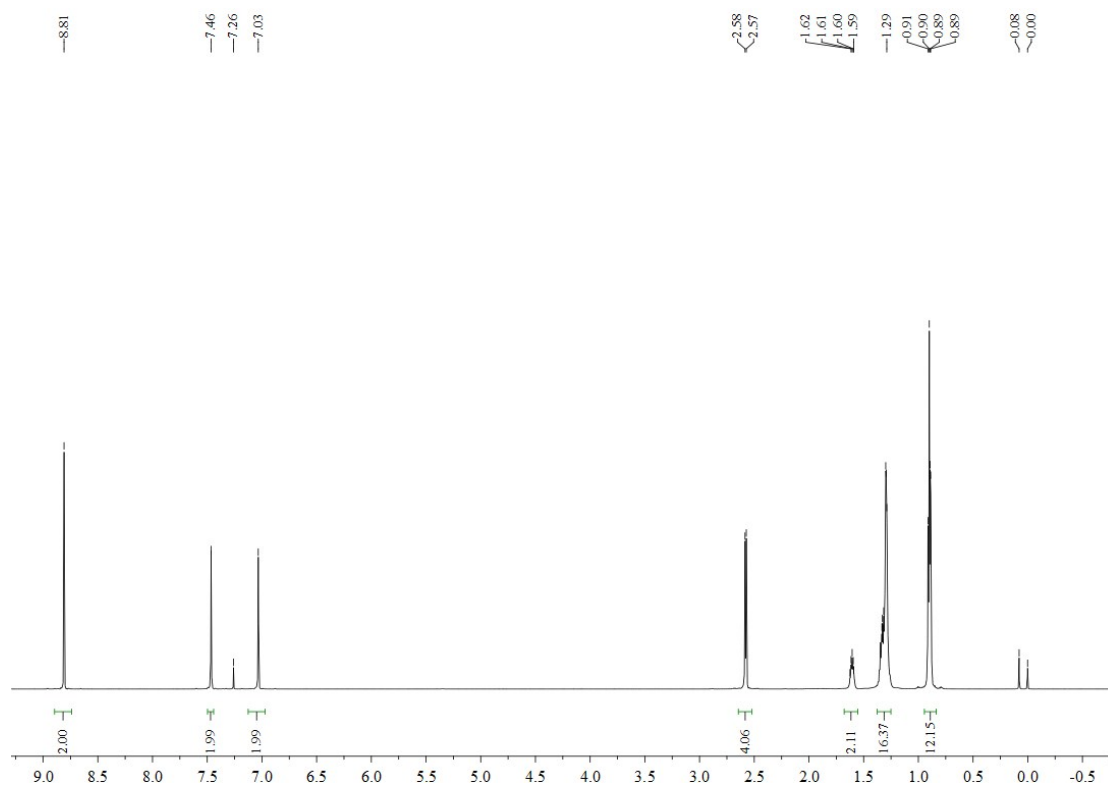


Fig. S6. ^1H NMR spectrum of compound m1 (CDCl_3).

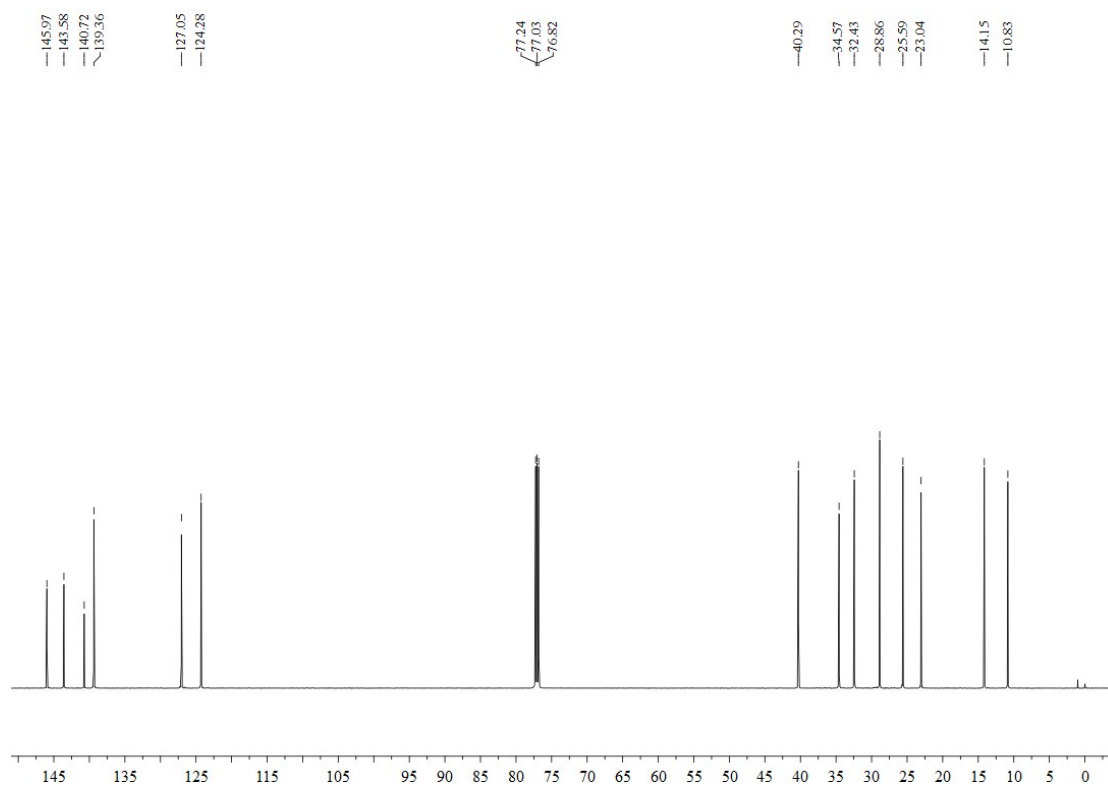


Fig. S7. ^{13}C NMR spectrum of compound m1 (CDCl_3).

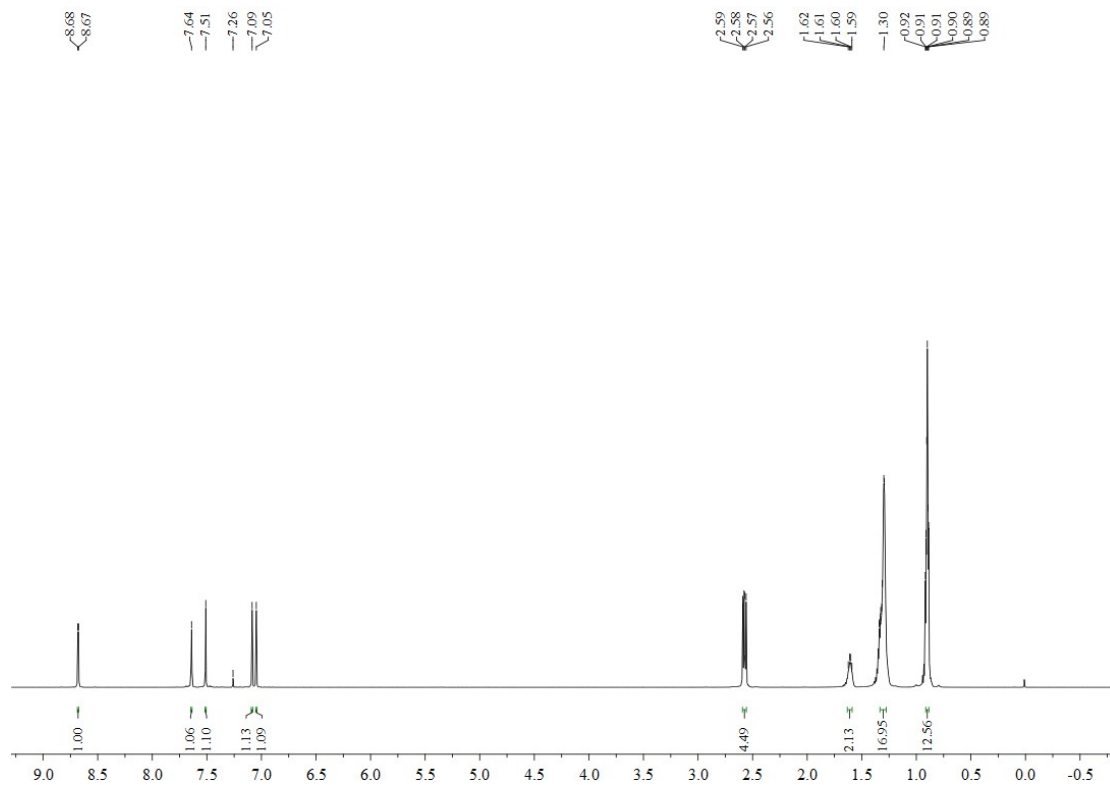


Fig. S8. ^1H NMR spectrum of compound m2 (CDCl_3).

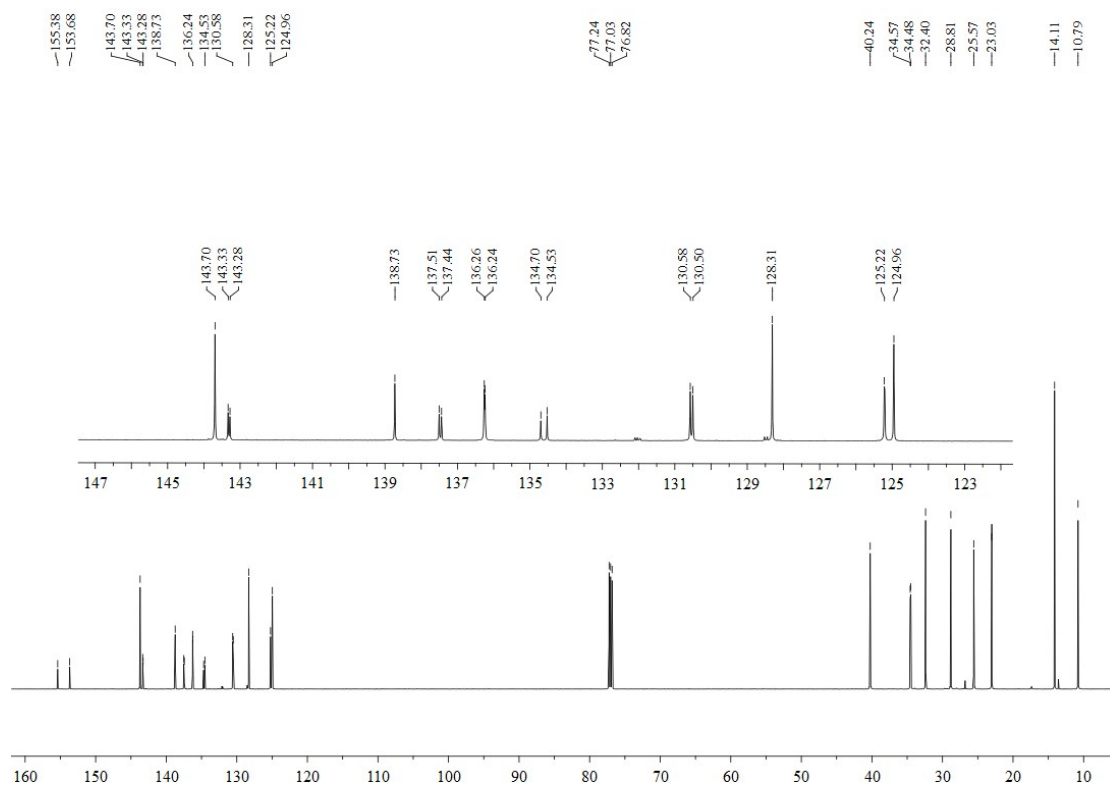


Fig. S9. ^{13}C NMR spectrum of compound m2 (CDCl_3).

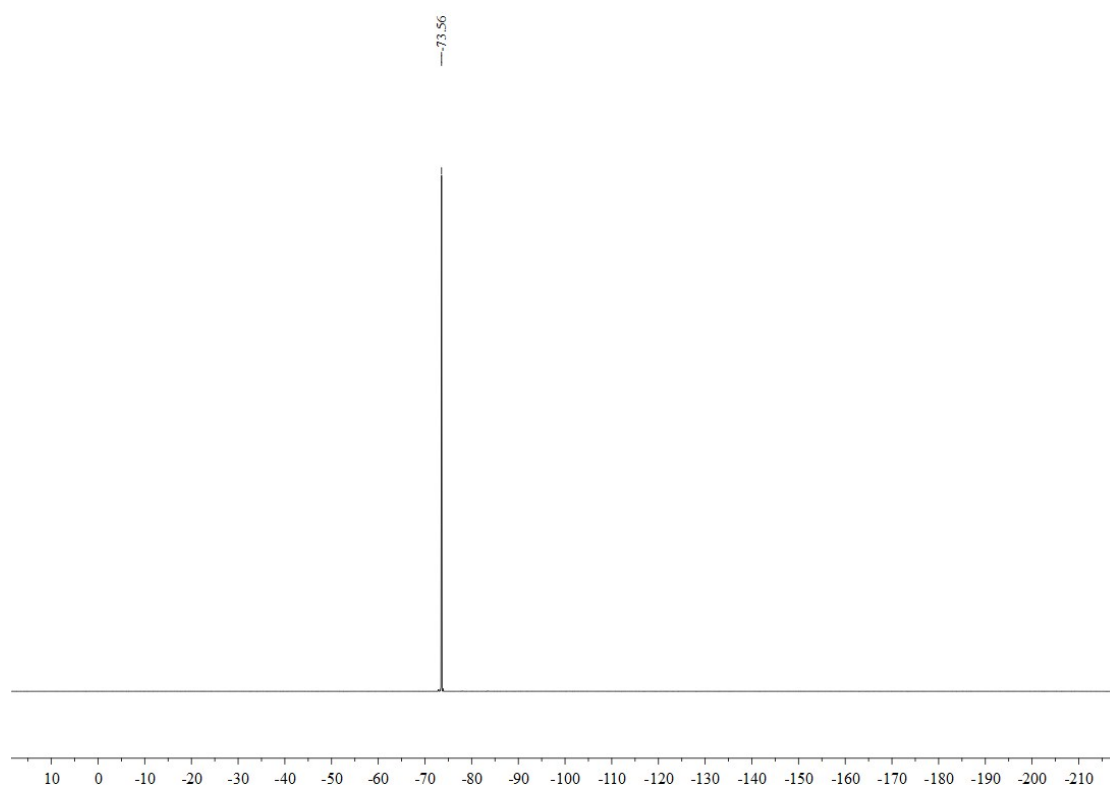


Fig. S10. ^{19}F NMR spectrum of compound m2 (CDCl_3).

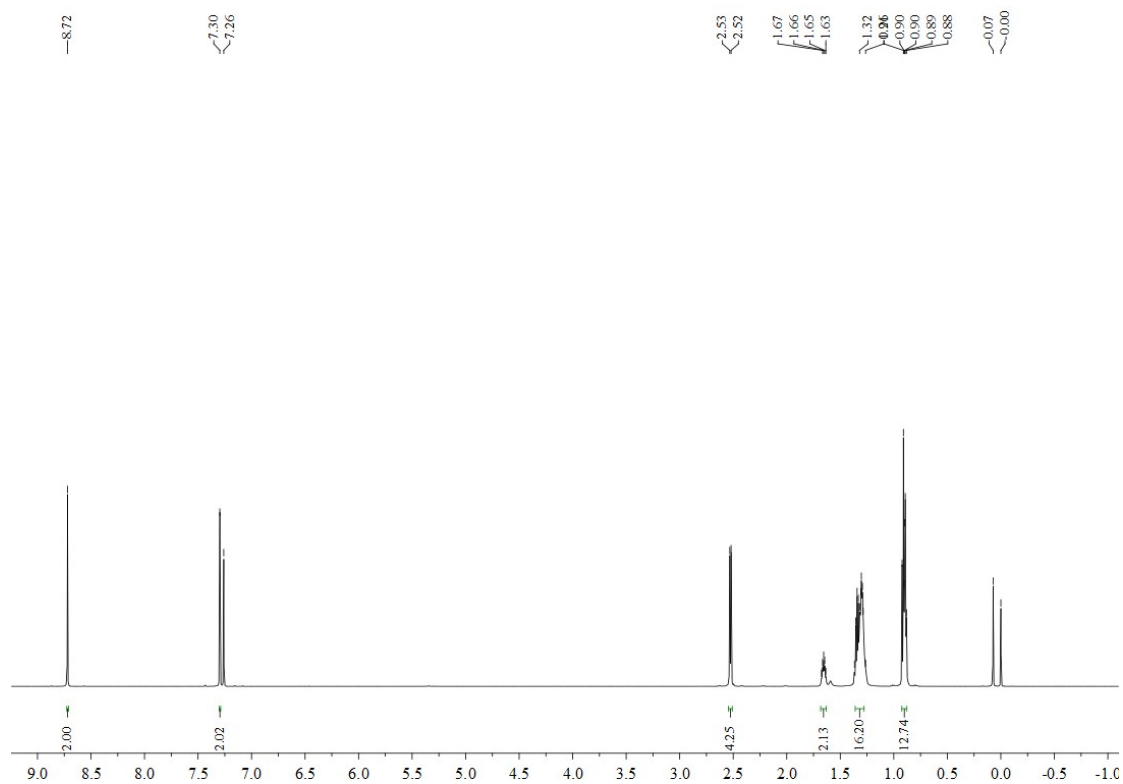


Fig. S11. ^1H NMR spectrum of compound M1 (CDCl_3).

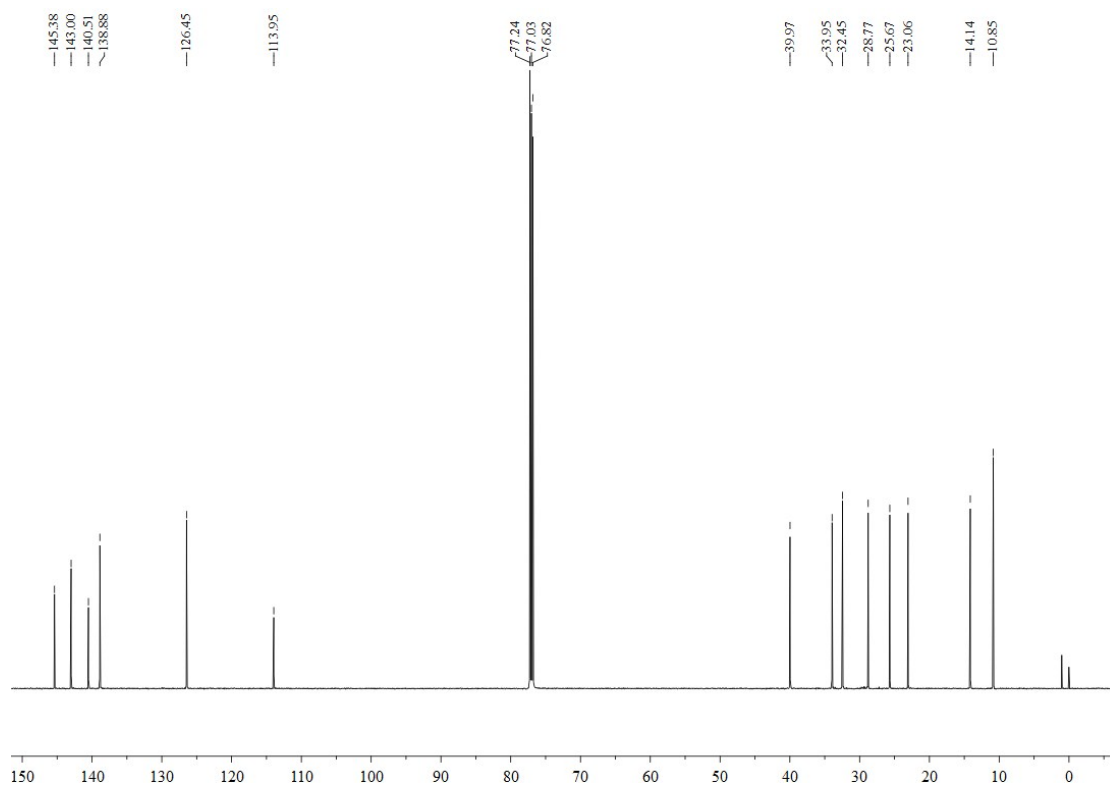


Fig. S12. ^{13}C NMR spectrum of compound M1 (CDCl_3).

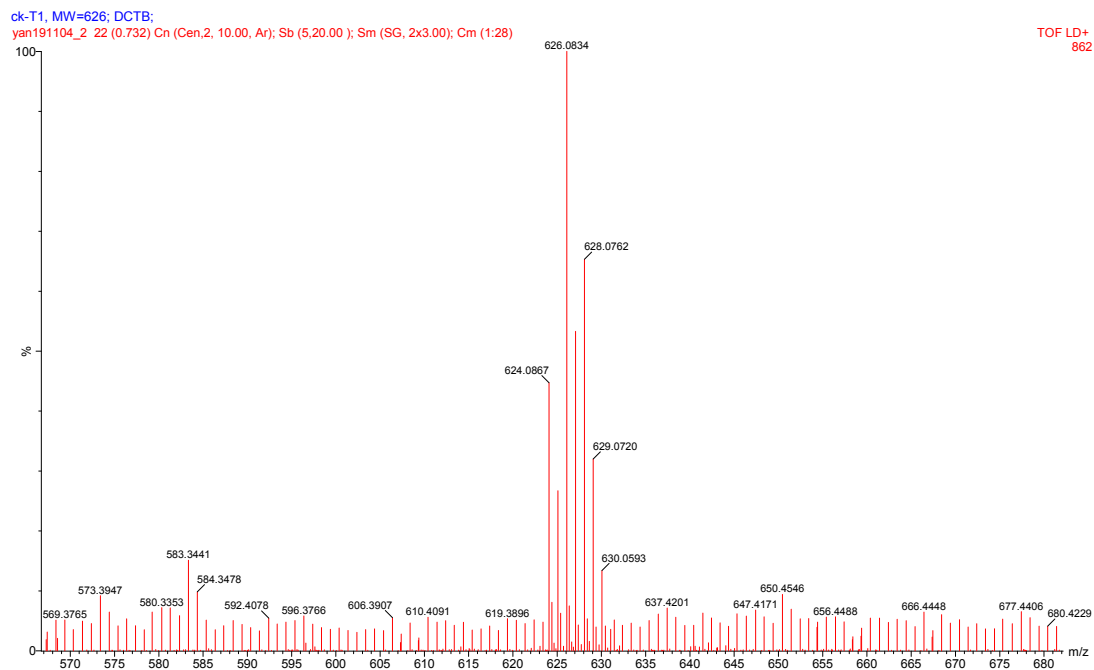


Fig. S13. MALDI-TOF MS spectrum of compound M1.

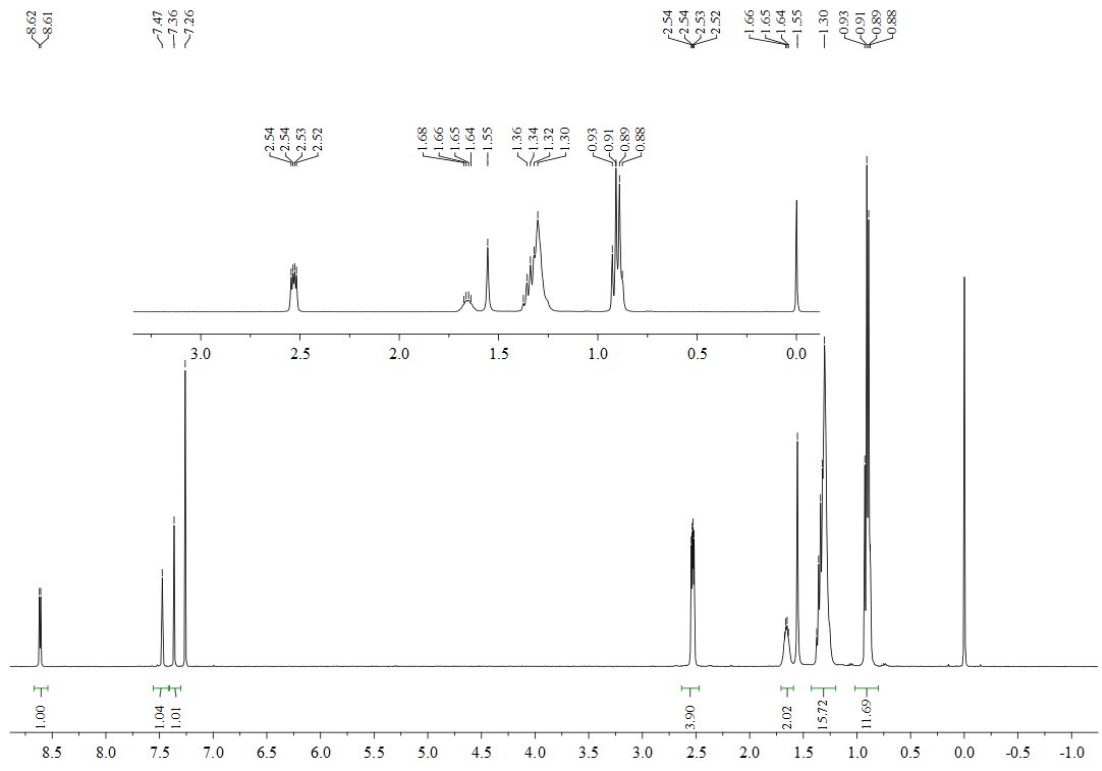


Fig. S14. ¹H NMR spectrum of compound M2 (CDCl₃).

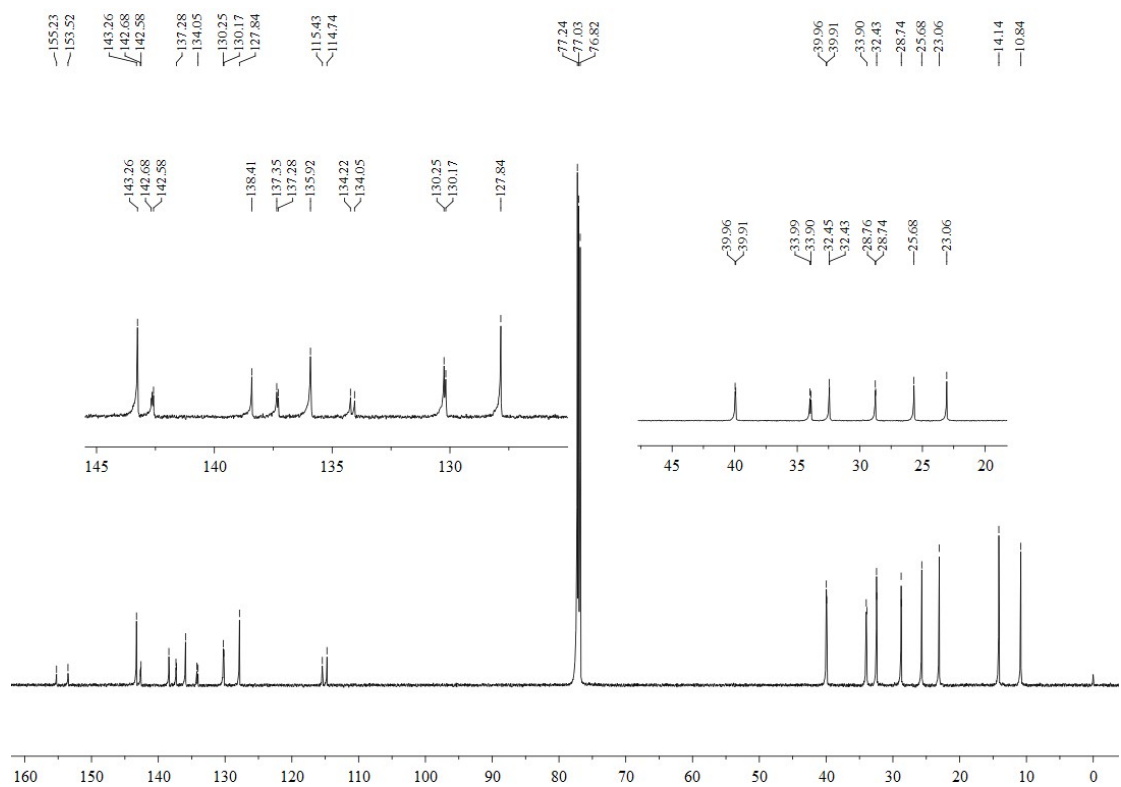


Fig. S15. ¹³C NMR spectrum of compound M2 (CDCl₃).

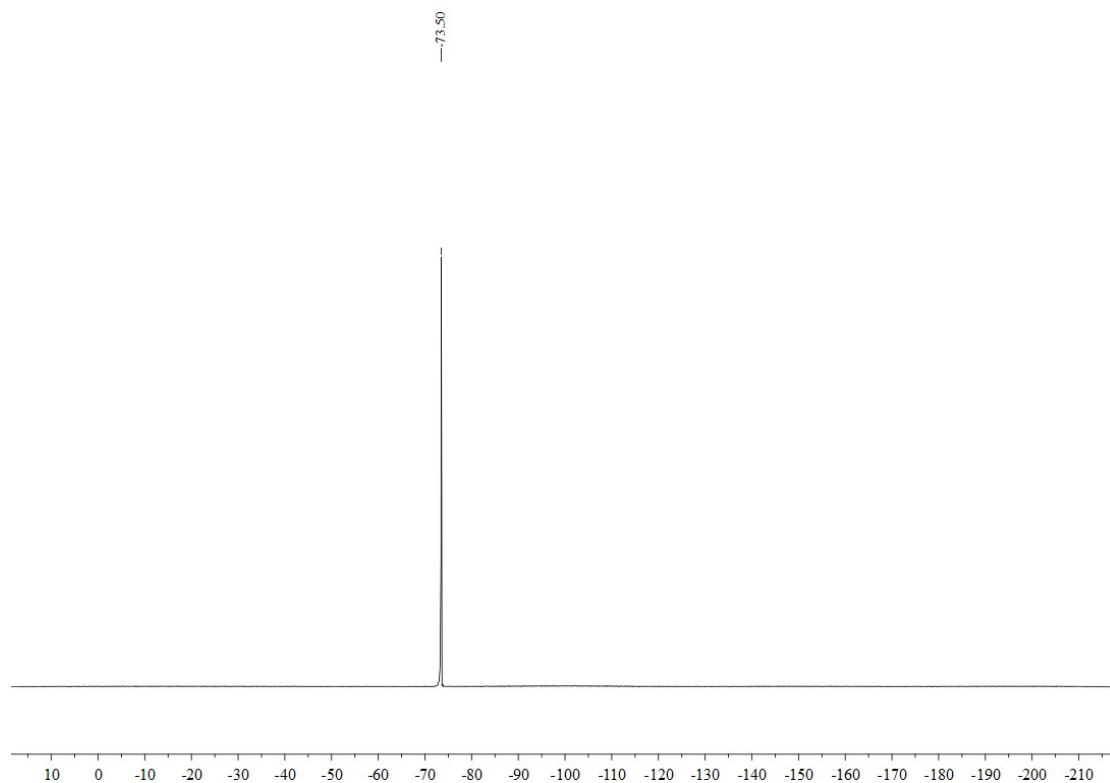


Fig. S16. ^{19}F NMR spectrum of compound M2 (CDCl_3).

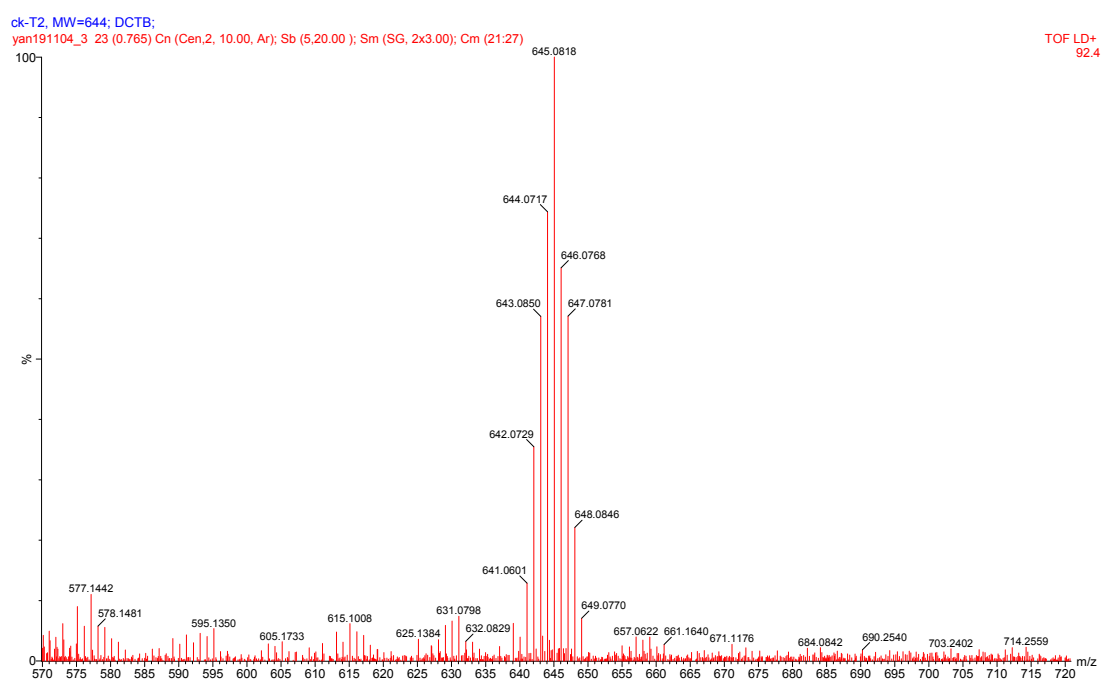


Fig. S17. MALDI-TOF MS spectrum of compound M2.